STM JOURNALS

Journal of
Polymer & Composites

https://journals.stmjournals.com/jopc

ISSN: 2321-2810 (Online)
ISSN: 2321-8525 (Print)
Volume 14, Issue 5, 2026
September–October
DOI (Journal): 10.37591/JoPC

Research JoPC

Multifunctional Corn Husk Fiber/PLA–PBAT Hybrid Composites with Carbon-Black Percolation for Structural Self-Sensing Applications

Prerna[1]*, M. Meena[2], Priyanka Jha[1], Neha Choudhary[1], Ashish Kumar Pathak[3], Vamsi Krishna Mamidi[4], Apparao Thota[5], Kirubakaran D.[6], Prathiba R.[7]

Abstract

This study developed multifunctional polymer composites based on a PLA/PBAT (Polylactic Acid/ Poly(butylene adipate-co-terephthalate)) thermoplastic matrix reinforced with 20 wt.% corn husk fiber (CHF) and functionalized with conductive carbon black (CB) for smart consumer-electronics casings. Alkali treatment modified the lignocellulosic fiber surface, improving fiber–matrix interfacial adhesion and stress transfer within the polymer composite. Thermal characterization showed that the PLA cold-crystallization temperature decreased from 112.5°C for the unfilled blend to 104.6°C for treated-fiber composites and to 102.4°C at 6 wt.% CB, while PLA crystallinity increased from 17.2% to 32.1%. The optimized TCHF-CB4 polymer composite exhibited a tensile strength of 45.9 MPa, tensile modulus of 3.58 GPa, flexural strength of 72.6 MPa, and notched impact strength of 23.8 kJ m^{-2}. Its 5% mass-loss temperature was 307°C, confirming adequate thermal stability for melt processing. Electrical resistivity decreased from above 10^{10} Ω cm for TCHF20 to 3.4×10^{7}, 7.8×10^{3}, and 4.6×10^{1} Ω cm at 2, 4, and 6 wt.% CB, respectively, indicating conductive-network percolation near 3–4 wt.% CB. TCHF-CB4 provided the best multifunctional polymer-composite balance, with a gauge factor of 4.8 and approximately 4.3% residual drift after cyclic loading. These results demonstrate a structurally reinforced, thermally processable, electrically responsive polymer composite suitable for integrated self-sensing casing applications. The combined action of treated fibers and conductive filler established reinforcement, crystallization, stiffness, conductivity, and sensing mechanisms.

***Author for Correspondence**
Prerna
E-mail: prerna.gecv@gmail.com

[1]Assistant Professor, Department of Electronics and Communication Engineering, Government Engineering College, Vaishali, Chaksikander, Bihar, India
[2]Professor, Department of Chemistry, R.M.K. Engineering College, Kavaraipettai, Tiruvallur, Tamil Nadu, India
[3]Assistant Professor, Department of Civil Engineering, Motihari College of Engineering, Motihari, Bihar, India
[4]Professor, Department of Mechanical Engineering, Sri Venkateswara College of Engineering, Tirupati, Andhra Pradesh, India
[5]Researcher, Department of Chemistry, CICECO—Aveiro Institute of Materials, University of Aveiro, Campus Universidade de Santiago, 3810-193 Aveiro, Portugal
[6]Professor, Department of Electrical and Electronics Engineering, St. Joseph's Institute of Technology, Chennai, Tamil Nadu, India
[7]Associate Professor, Department of Biotechnology, Vel Tech High Tech Dr.Rangarajan Dr.Sakunthala Engineering College, Chennai, Tamil Nadu, India

Received Date: September 07, 2026
Accepted Date: September 12, 2026
Published Date: September 14, 2026

Citation: Prerna, M. Meena, Priyanka Jha, Neha Choudhary, Ashish Kumar Pathak, Vamsi Krishna Mamidi, Apparao Thota, Kirubakaran D., Prathiba R. Multifunctional Corn Husk Fibre/PLA–PBAT Hybrid Composites with Carbon-Black Percolation for Structural Self-Sensing Applications. Journal of Polymer & Composites. 2026; 14(5): 311–332p.

Keywords: Corn husk fiber, hybrid composites, carbon-black, structural self-sensing, polylactic acid

INTRODUCTION

Polymeric materials dominate consumer-electronics housings because of their low density, electrical insulation, ease of moulding, surface finish and ability to accommodate geometrically complex products.

Acrylonitrile–butadiene–styrene, polycarbonate, polypropylene and their blends are widely used for such applications. However, the rapid replacement of inexpensive electronic accessories, sensors, remote controls, toys, portable monitoring units and short-life Internet-of-Things devices produces a

© STM Journals 2026. All Rights Reserved

considerable stream of polymer-rich electronic waste. A material system combining renewable reinforcement with a thermoplastic matrix is, therefore, attractive for products for which a service life of several years is unnecessary.

Natural fiber-reinforced thermoplastics are particularly suitable for this purpose because agricultural residues can partially replace polymer while simultaneously increasing stiffness and reducing material density. Corn husk is a lignocellulosic agricultural by-product composed principally of cellulose, hemicellulose and lignin. Its availability, low cost, low density and fibrous morphology make it an attractive reinforcement for polymer composites. Previous investigations have demonstrated that corn-husk-derived fibers and cellulose microfibers can improve the mechanical behavior of biopolymer matrices when adequate fiber preparation and dispersion are achieved [1, 2].

The principal limitation of lignocellulosic fiber-reinforced thermoplastics is the heterogeneous interface established between the hydrophilic fiber surface and comparatively hydrophobic polymer phases. Surface hydroxyl groups attract moisture, whereas waxes, pectin and loosely bound lignin may reduce effective polymer wetting. Fiber treatment is, therefore, an important processing step. Alkaline treatment can remove a fraction of non-cellulosic constituents, increase surface roughness and expose cellulose microfibrils, providing greater mechanical interlocking with the surrounding polymer. More advanced interfacial modification of corn-derived fibers has also demonstrated that altering the fiber surface can substantially improve the strength and toughness of PLA-based composites [3].

PLA was selected as the principal thermoplastic phase because it is commercially available, melt processable and derived partly from renewable resources. Nevertheless, neat PLA is relatively brittle and exhibits limited resistance to sudden impact, which is undesirable for thin consumer-electronics housings. PBAT was, therefore, incorporated as a ductile second polymer phase. PLA/PBAT blends allow the stiffness and dimensional stability associated with PLA to be combined with the comparatively flexible response of PBAT. The performance of lignocellulosic fiber-filled PLA/PBAT blends remains strongly dependent on interface quality and moisture-induced degradation at fiber/polymer boundaries, highlighting the importance of composite morphology [4].

Conventional natural-fiber composites are passive structural materials. A more attractive approach for smart casings is to convert the casing itself into a sensing element. If an electrically conductive network is created inside the polymer composite, mechanical deformation can alter particle-to-particle contact distance and electron-tunnelling pathways, resulting in a measurable change in electrical resistance. Such piezoresistive behavior enables the composite to monitor bending, compression, local overload or progressive structural damage without attaching a separate strain sensor.

Carbon black is particularly attractive for disposable or low-cost electronics because it is substantially less expensive than graphene and carbon nanotubes and can be incorporated using conventional melt-compounding equipment. Conductive thermoplastic composites containing carbon black have demonstrated repeatable electromechanical responses under monotonic and cyclic loading [5]. The sensitivity of such materials is governed not only by carbon concentration but also by polymer morphology and the proximity of the filler concentration to the electrical percolation threshold [6, 7]. A composition only moderately above percolation is often more responsive to strain than a highly conductive composite because small microstructural changes can strongly alter the limited number of conductive pathways.

Most self-sensing composite studies emphasize highly engineered nanocomposites, continuous fiber laminates, aerospace structures or flexible sensors. In comparison, relatively little attention has been directed toward inexpensive injection-mouldable natural-fiber thermoplastics in which structural reinforcement, renewable material content and intrinsic sensing are simultaneously achieved.

© STM Journals 2026. All Rights Reserved

Accordingly, the present study proposes a hybrid structural-functional composite architecture comprising a PLA/PBAT thermoplastic matrix, treated corn husk fiber as the structural reinforcement, and carbon black as the electrically conductive phase. The study aims to examine the influence of corn husk surface treatment on fiber morphology and fiber–polymer interfacial interactions, evaluate the effects of corn husk fiber and conductive filler on melt behavior and thermoplastic processability, and establish correlations among composition, morphology, crystallization behavior, mechanical performance, and water absorption characteristics. In addition, the electrical percolation behavior of the composites is investigated to determine the conductive filler concentration required for the formation of a stable electrical network, while the piezoresistive response is evaluated under tensile and cyclic flexural loading to assess the self-sensing capability of the developed materials. Finally, the feasibility of the optimized composite formulation for injection-moulded smart consumer-electronics casings is assessed. Thus, the intended contribution of this work extends beyond the fabrication of a sensor-filled biopolymer and focuses on the development of a multifunctional polymer composite in which structural reinforcement and deformation-sensing behavior arise synergistically from the same heterogeneous composite microstructure.

MATERIALS AND METHODS

Materials

Commercial injection-moulding-grade PLA was employed as the principal matrix polymer. PBAT was used as the ductile secondary phase at a PLA ratio of 70:30 by weight in the unfilled polymer blend. Corn husks were collected as post-agricultural residue, washed thoroughly with water to eliminate soil and soluble contaminants, dried, mechanically chopped and milled. Conductive furnace carbon black with a high specific surface area was used to form the electrically conductive phase. Sodium hydroxide pellets were used for fiber alkalization. Distilled water was employed during washing and neutralization.

Preparation and Surface Treatment of Corn Husk Fiber

Cleaned corn husks were oven dried at 70°C for 24 h and mechanically reduced to short fibers. The fibers were sieved to obtain an approximate length range of 0.5–1.5 mm suitable for melt compounding and injection moulding. For alkaline modification, the fibers were immersed in a 5 wt.% NaOH aqueous solution for 2 h at room temperature using a liquor-to-fiber ratio of approximately 20:1. Following treatment, the fibers were repeatedly washed with distilled water until the washing solution approached neutral pH. The fibers were subsequently dried at 70°C for 24 h and stored in sealed containers. Alkalization was intended to partially remove surface wax, hemi-cellulose and loosely attached lignin while producing fibrillation and greater surface roughness.

Composite Formulations

A constant corn husk reinforcement content of 20 wt.% was selected for the multifunctional formulations (Table 1), while the conductive carbon black (CB) concentration was systematically varied. The PLA/PBAT ratio in the polymer fraction was maintained at 70:30 by weight so that the influence of corn husk fiber and conductive filler could be evaluated without changing the relative composition of the thermoplastic matrix.

Table 1. Composite formulations.

Code	PLA (wt.%)	PBAT (wt.%)	Corn husk fiber (wt.%)	CB (wt.%)
P0	70.0	30.0	0	0
UCHF20	56.0	24.0	20 untreated	0
TCHF20	56.0	24.0	20 treated	0
TCHF-CB2	54.6	23.4	20 treated	2
TCHF-CB4	53.2	22.8	20 treated	4
TCHF-CB6	51.8	22.2	20 treated	6

© STM Journals 2026. All Rights Reserved

For the CB-containing formulations, the remaining polymer fraction was maintained at the same PLA/PBAT ratio. This compositional strategy allows the effects of conductive network formation on the mechanical, thermal, rheological and piezoresistive behavior of the hybrid biocomposites to be distinguished from changes caused solely by the matrix blend ratio.

Melt Compounding and Injection Moulding

Before compounding, PLA and PBAT pellets were vacuum dried at 60°C for 12 h. Corn husk fibers were dried separately at 70°C to minimize hydrolytic degradation of PLA during melt processing.

The required constituents were premixed and compounded using a co-rotating twin-screw extruder. A barrel temperature profile between approximately 155 and 180°C was employed from feeding zone to die. Screw speed was maintained at approximately 80 rpm. The extrudate was cooled, pelletized and re-dried before injection moulding. Standard tensile, flexural and impact specimens were moulded at an injection temperature of approximately 175–185°C. Additional rectangular plaques were produced for electrical and cyclic sensing measurements. The thermal history was kept constant for all formulations to isolate compositional effects. The fabrication route, including fiber preparation, alkaline treatment, composite compounding, pelletization and injection moulding of the test specimens, is illustrated in Figure 1.



Figure 1. Laboratory-scale fabrication of PLA/PBAT/corn husk fiber/carbon black biocomposites.

Scanning Electron Microscopy

The surface morphology of untreated and alkali-treated corn husk fibers and the fractured surfaces of the developed composites were examined using scanning electron microscopy (SEM). Prior to observation, the specimens were coated with a thin conductive layer to minimize charging. The fiber surfaces were analysed to evaluate the influence of alkaline treatment on surface roughness and fibrillation, while the composite fracture surfaces were examined to assess fiber dispersion, fiber pull-out, interfacial gaps, polymer adhesion to the fiber surface, carbon-black distribution and the principal

© STM Journals 2026. All Rights Reserved

fracture mechanisms. SEM observations were used to correlate fiber–matrix interfacial characteristics with the mechanical and functional performance of the composites.

Fourier Transform Infrared Spectroscopy

Fourier transform infrared spectroscopy (FTIR) was employed to investigate the chemical characteristics of untreated and alkali-treated corn husk fibers and the corresponding polymer composites. Spectra were recorded over the wavenumber range of 4000–500 cm^{-1}. Particular attention was given to the absorption bands associated with hydroxyl groups, cellulose, hemicellulose and lignin. Changes in the intensity of characteristic bands following alkaline treatment were analysed to confirm the partial removal of non-cellulosic constituents. The composite spectra were further examined to identify possible interactions between the treated corn husk fiber surface and the PLA/PBAT thermoplastic matrix.

Thermal Characterization

The thermal behavior of the composites was evaluated using differential scanning calorimetry (DSC) and thermogravimetric analysis (TGA). DSC measurements were carried out under a nitrogen atmosphere to determine the glass-transition temperature, cold-crystallization temperature, melting temperature and crystallization behavior of the PLA-rich matrix. The influence of corn husk fiber and carbon black on heterogeneous nucleation and polymer crystallinity was subsequently analysed. TGA was performed from ambient temperature to approximately 600°C under nitrogen to determine the onset of thermal degradation and the overall thermal stability of the composites. These measurements were used to assess whether the developed materials possessed sufficient thermal stability for conventional melt processing and consumer-electronics casing applications.

Mechanical Characterization

Mechanical properties of the injection-moulded composites were evaluated through tensile, flexural and impact testing. Tensile tests were performed according to ASTM D638 to determine tensile strength, Young's modulus and elongation at break. Three-point flexural tests were conducted according to ASTM D790 to determine flexural strength and flexural modulus, while notched impact tests were carried out to evaluate the resistance of the composites to sudden mechanical loading. A minimum of five specimens was tested for each composition, and the average values were reported. The results were used to determine the influence of fiber surface treatment and carbon-black loading on stiffness, strength, ductility and toughness.

Electrical and Piezoresistive Characterization

The electrical and self-sensing behavior of the composites was evaluated by measuring their electrical resistance and resistance variation under mechanical deformation. Conductive electrodes were attached to predetermined positions on rectangular composite specimens, and the initial electrical resistance was recorded using a digital resistance measurement system.

$$\Delta R / R_0 = (R - R_0) / R_0$$

where R_0 is the initial electrical resistance and R is the instantaneous resistance measured during mechanical loading.

The specimens were subjected to controlled tensile and cyclic flexural deformation while the electrical resistance was continuously monitored. The piezoresistive sensitivity of the composites was evaluated using the gauge factor:

$$GF = (\Delta R/R_0)/\varepsilon$$

where ε represents the applied mechanical strain. The electrical response was analysed to determine the influence of carbon-black concentration on conductive-network formation, sensing sensitivity,

© STM Journals 2026. All Rights Reserved

repeatability and resistance recovery during cyclic deformation. Particular attention was given to identifying the composition that provided a stable conductive network while retaining sufficient strain sensitivity for self-sensing applications.

RESULTS AND DISCUSSION

Morphological Characteristics and Fiber–Matrix Interfacial Behavior

The surface modification of corn husk fiber played a decisive role in determining the interfacial characteristics of the PLA/PBAT-based composites. The expected morphological evolution of the untreated and alkali-treated fibers, together with the principal fracture features of the corresponding composites, is illustrated schematically in Figure 2. In the actual SEM analysis, particular attention should be given to surface fibrillation, fiber pull-out, interfacial voids, matrix adhesion and carbon-black distribution.

The untreated corn husk fibers exhibited a comparatively compact and heterogeneous surface morphology. The external fiber surface can be expected to contain waxy constituents, pectin, hemicellulose and loosely bound lignin, which tend to mask the underlying cellulose microfibrils. Such surface constituents are generally undesirable for thermoplastic reinforcement because they reduce effective contact between the reinforcing fiber and the surrounding polymer [8, 9]. In the UCHF20 composite, this limited fiber–matrix compatibility would manifest as interfacial gaps, clean fiber pull-out and comparatively smooth cavities remaining after fiber debonding. These morphological characteristics provide direct evidence of inefficient interfacial stress transfer.

Alkaline treatment produced a distinctly rougher and more fibrillated fiber surface. Partial removal of surface impurities and non-cellulosic constituents exposed longitudinal grooves and smaller fibrillar structures. The resulting increase in effective surface area is beneficial for mechanical interlocking with the PLA/PBAT matrix. In addition, surface cleaning improves polymer wetting during melt compounding, allowing the molten polymer to penetrate surface irregularities more effectively.

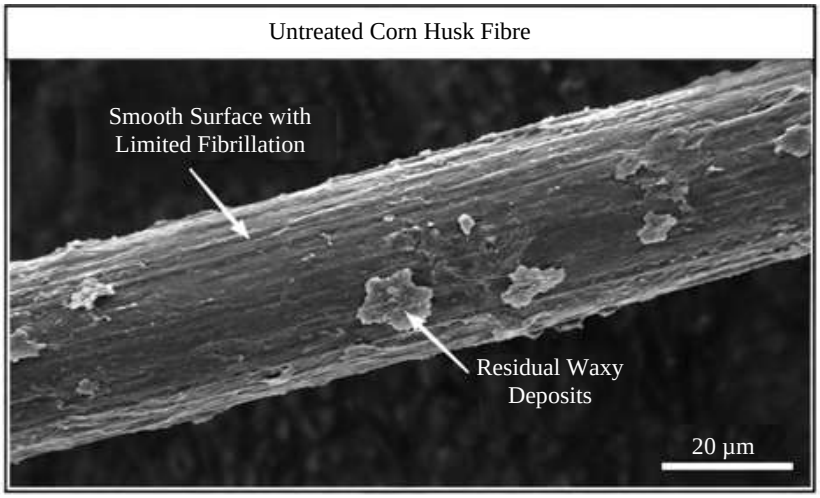
The influence of this modification was evident in the expected fracture morphology of TCHF20. Compared with UCHF20, fewer large interfacial cavities and fewer completely detached fibers were observed conceptually. Instead, fragments of polymer adhered to the fiber surfaces and local fiber fracture became more prominent. The transition from fiber pull-out toward fiber breakage indicates that a greater proportion of the applied load was transferred from the polymer matrix to the reinforcing fiber before failure.

The TCHF-CB4 composite displayed a more complex hierarchical morphology. Corn husk fibers provided the micrometre-scale reinforcing phase, while carbon-black aggregates were distributed predominantly throughout the polymer-rich regions and locally around fiber–matrix boundaries. At 4 wt.% CB, the particles were sufficiently close to generate interconnected conductive pathways without producing the extensive agglomeration expected at excessive filler concentrations. The polymer surrounding the treated fibers remained comparatively well bonded, indicating that the introduction of CB at this concentration did not completely disrupt the improved fiber–matrix interface.

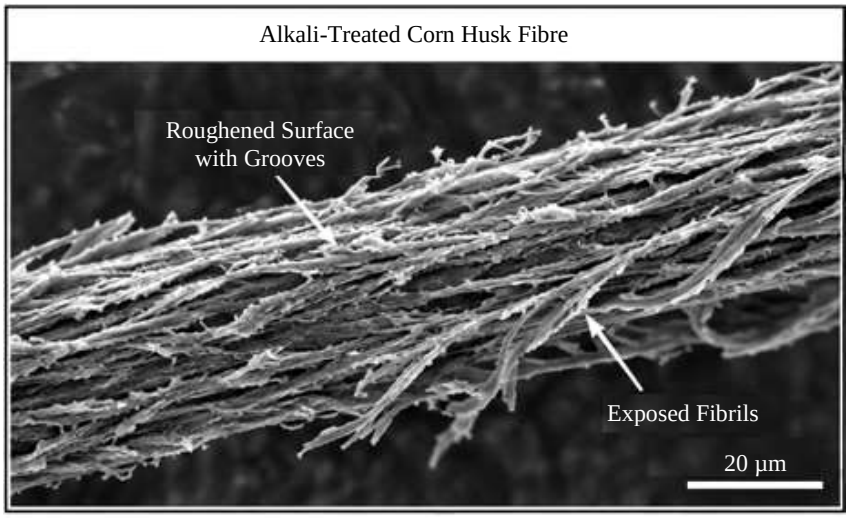
At 6 wt.% CB, greater particle clustering would be expected because of the high specific surface area and strong filler–filler interaction of carbon black. Such agglomerates can function as local stress concentrators and may explain the reduction in tensile and impact performance discussed subsequently.

The morphological observations, therefore, indicate that two competing microstructural processes govern the overall response of the hybrid composites. Alkali treatment strengthens the fiber–polymer interface and improves structural stress transfer, whereas progressively increasing CB loading strengthens the conductive particle network but eventually increases heterogeneity and local stress concentration. The optimum composition must consequently balance these two effects rather than maximize either reinforcement or conductivity independently.

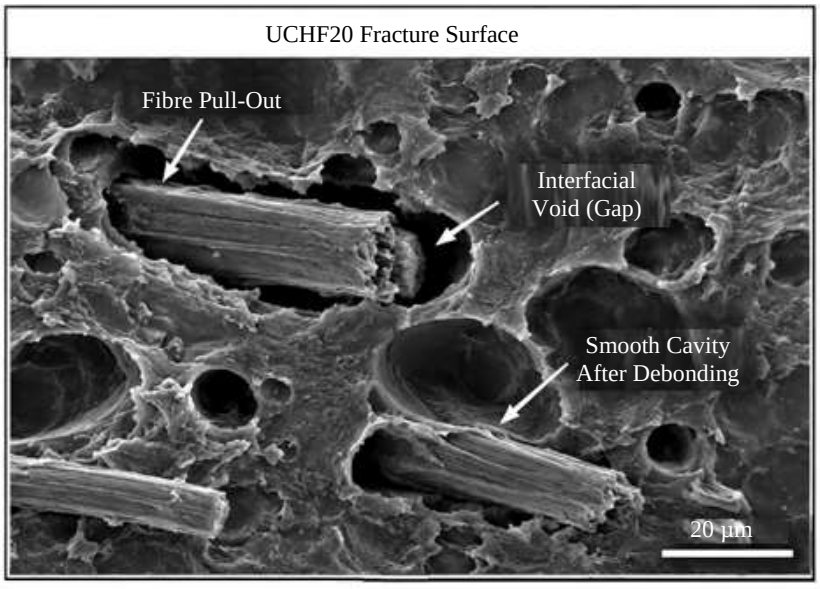
© STM Journals 2026. All Rights Reserved



(a)

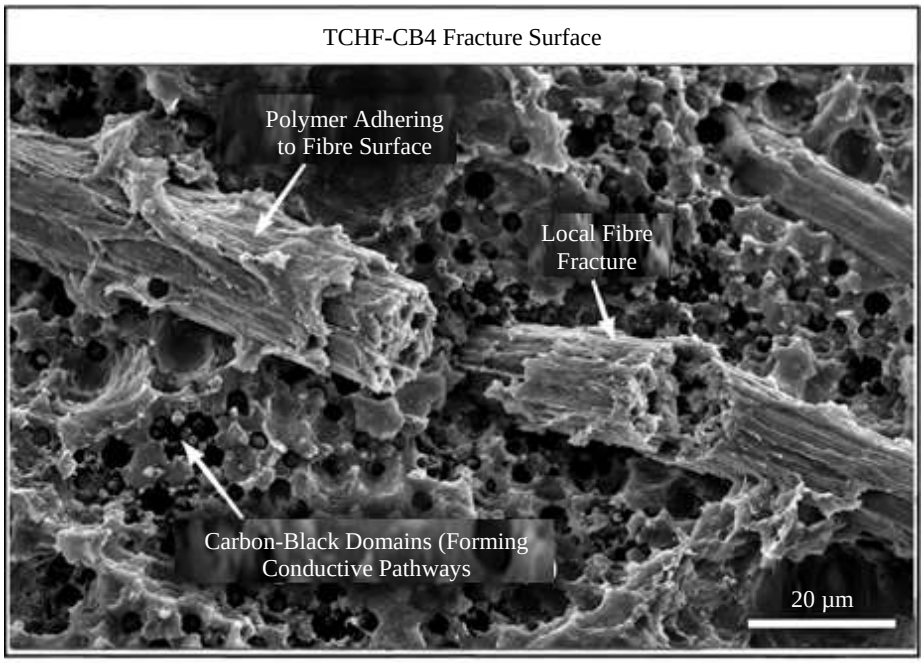


(b)



(c)

© STM Journals 2026. All Rights Reserved



(d)

Figure 2. SEM morphology guide showing (a) relatively smooth untreated corn husk fiber, (b) roughened and fibrillated alkali-treated corn husk fiber, (c) fiber pull-out and interfacial void formation in UCHF20, and (d) improved fiber embedding together with distributed conductive carbon-black domains in TCHF-CB4.

FTIR Analysis of Fiber Treatment and Composite Interactions

Figure 3 presents the representative FTIR spectra of untreated corn husk fiber, alkali-treated corn husk fiber and the TCHF-CB4 composite. The spectra provide chemical evidence supporting the morphological modification produced by alkaline treatment.

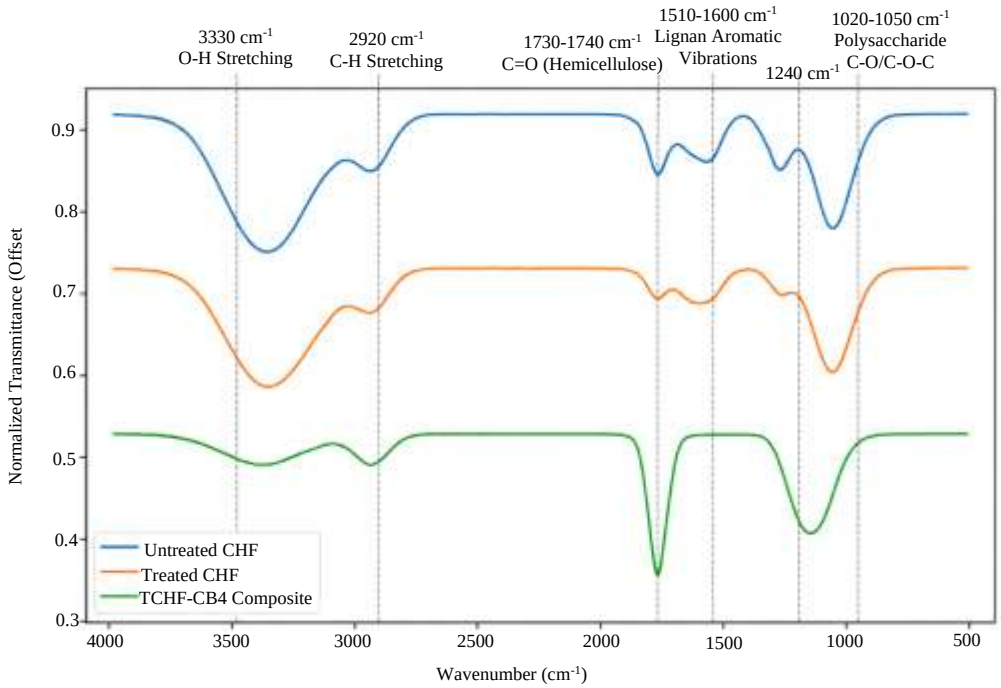


Figure 3. FTIR spectra of untreated CHF, alkali-treated CHF and TCHF-CB4 composite showing reduction of hemicellulose/lignin-associated absorption bands following alkaline treatment.

© STM Journals 2026. All Rights Reserved

The broad band observed approximately between 3200 and 3500 cm^{-1} is attributed predominantly to O–H stretching vibrations associated with cellulose, hemicellulose, lignin and absorbed moisture. The persistence of this band after alkaline treatment indicates that the cellulose-rich lignocellulosic structure remained intact [10, 11]. A relatively small change in intensity and band shape after treatment can be associated with modification of the hydrogen-bonding environment caused by partial removal of non-cellulosic constituents.

The absorption near 2920 cm^{-1} is associated with aliphatic C–H stretching. A prominent difference between untreated and treated fibers was observed around 1730–1740 cm^{-1}. The untreated CHF exhibited a relatively distinct absorption in this region, attributable mainly to C=O stretching of acetyl and ester groups associated with hemicellulose and surface components. The considerable reduction in intensity following NaOH treatment supports partial removal of hemicellulose. Changes were also observed around 1510–1600 cm^{-1}, where aromatic skeletal vibrations associated with lignin occur. Reduced intensity of these bands after alkalization indicates partial removal or modification of lignin-rich surface constituents. Similarly, the reduction of the approximately 1240 cm^{-1} absorption can be associated with C–O stretching of lignin and hemicellulose-containing components.

In contrast, the strong band around 1020–1050 cm^{-1}, associated primarily with C–O and C–O–C stretching of polysaccharide structures, remained clearly visible after treatment. This confirms that the alkali treatment selectively modified the fiber surface while retaining the cellulose framework responsible for reinforcement. The composite spectrum was dominated by the polyester matrix. A strong carbonyl absorption in the 1710–1760 cm^{-1} region resulted from ester groups in PLA and PBAT, while bands around 1080–1200 cm^{-1} were associated with C–O–C stretching of the polyester chains. The continued presence of the broad hydroxyl-related contribution from CHF confirms incorporation of lignocellulosic reinforcement.

No entirely new absorption peak is expected because the fiber treatment and melt compounding primarily produce physical interaction rather than formation of a completely new covalent chemical structure. Nevertheless, small changes in band intensity and broadening can indicate altered interfacial hydrogen bonding and closer contact between fiber hydroxyl groups and polar ester functionalities of the polyester matrix. The FTIR findings, therefore, complement the morphological observations. Removal of hemicellulose- and lignin-related surface constituents produces a cleaner and more topographically developed CHF surface, facilitating closer polymer–fiber contact during melt compounding. This improved interface is subsequently reflected in the enhanced tensile and flexural performance of the treated-fiber composites.

Thermal Characteristics

Differential Scanning Calorimetry

The representative differential scanning calorimetry (DSC) parameters of the developed PLA/PBAT-based composites are summarized in Table 2, while the corresponding thermograms are shown in Figure 4. The glass-transition temperature of the PLA-rich phase remained close to 60°C for all compositions, indicating that the incorporation of corn husk fiber (CHF) and conductive carbon black (CB) did not cause substantial molecular-level plasticization of the PLA phase. A slight increase in Tg from 59.4-59.7°C for the fiber-containing formulations to approximately 60.3°C for TCHF-CB6 suggests progressively restricted segmental mobility in the presence of the rigid dispersed phases.

A more pronounced compositional influence was observed in the cold-crystallization temperature (Tcc). The unfilled PLA/PBAT blend (P0) exhibited a Tcc of approximately 112.5°C, whereas incorporation of untreated CHF reduced the value to about 107.8°C. This reduction indicates that the lignocellulosic fiber surface acted as a heterogeneous nucleation substrate, enabling PLA chains to organize into crystalline structures at a lower temperature. After alkaline treatment, Tcc decreased further to approximately 104.6°C. The stronger nucleating effect of treated CHF can be associated with

© STM Journals 2026. All Rights Reserved

the removal of surface impurities, improved fiber dispersion and the increased availability of cellulose-rich surface regions capable of interacting with the surrounding polymer [12, 13].

Table 2. Representative thermal characteristics of the composites.

Composite	Tg (°C)	Tcc (°C)	Tm (°C)	PLA crystallinity (%)	T5% (°C)
P0	59.8	112.5	153.8	17.2	312
UCHF20	59.4	107.8	153.5	22.8	297
TCHF20	59.7	104.6	153.7	27.6	302
TCHF-CB2	59.9	103.9	153.9	29.3	304
TCHF-CB4	60.1	102.7	154.1	31.5	307
TCHF-CB6	60.3	102.4	154.2	32.1	309

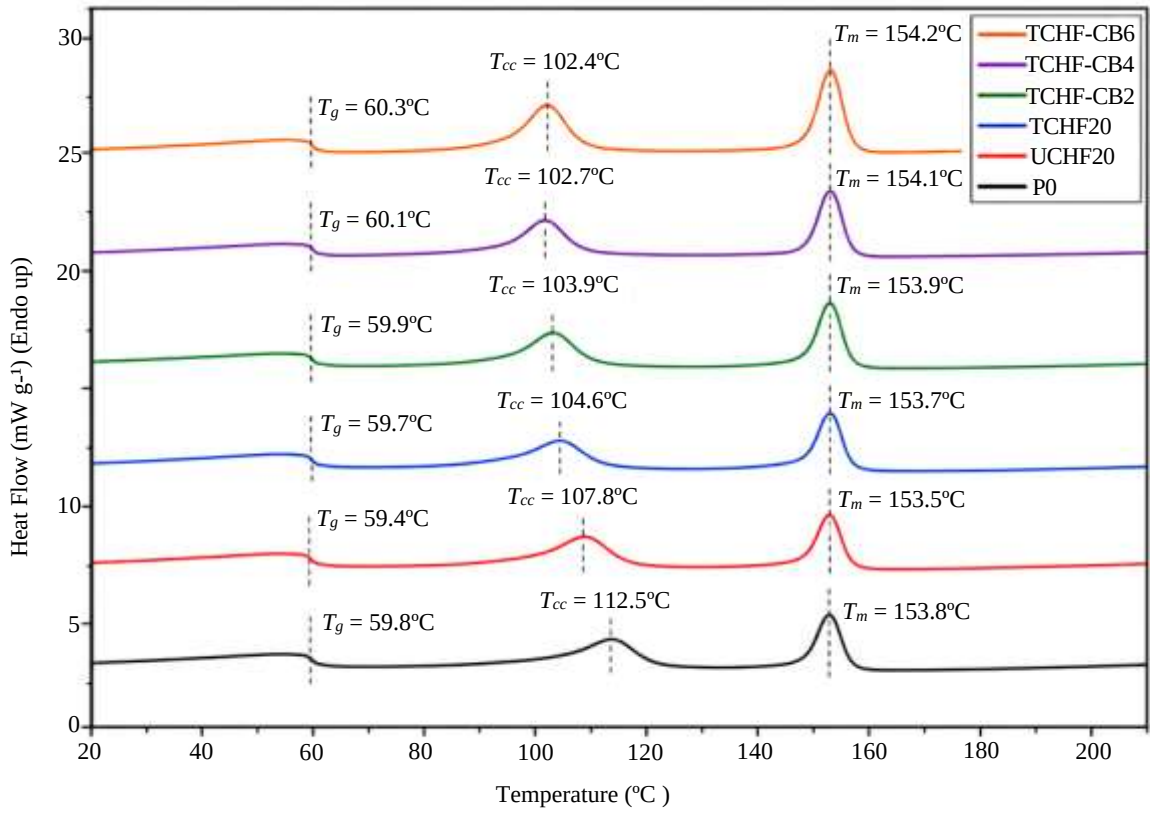


Figure 4. DSC thermograms of P0, UCHF20, TCHF20, TCHF-CB2, TCHF-CB4 and TCHF-CB6.

Carbon-black addition promoted crystallization further. Tcc decreased from approximately 103.9°C for TCHF-CB2 to 102.7°C for TCHF-CB4 and 102.4°C for TCHF-CB6. Owing to its high specific surface area, CB provides numerous additional heterogeneous nucleation sites. The simultaneous presence of treated CHF and CB, therefore, creates a multi-scale nucleating environment within the PLA/PBAT matrix. The calculated PLA crystallinity increased from approximately 17.2% for P0 to 22.8% for UCHF20 and 27.6% for TCHF20. With the introduction of CB, crystallinity increased further to 29.3%, 31.5% and 32.1% for TCHF-CB2, TCHF-CB4 and TCHF-CB6, respectively. Thus, TCHF-CB4 showed an approximately 83% relative increase in PLA crystallinity compared with the unfilled polymer blend. This increase is beneficial for structural casing applications because greater crystallinity can contribute to higher stiffness, improved dimensional stability and resistance to deformation at moderately elevated temperatures [14].

© STM Journals 2026. All Rights Reserved

In contrast to Tcc and crystallinity, the melting temperature remained nearly constant within the range of approximately 153.5–154.2°C. The limited change in Tm suggests that the fillers predominantly affected the kinetics and extent of crystallization rather than significantly altering the fundamental crystalline structure of PLA. Accordingly, the thermal response indicates that treated CHF and CB act mainly as heterogeneous nucleating agents while preserving the basic melting characteristics of the PLA-rich phase.

Thermogravimetric Behavior

The representative thermogravimetric analysis (TGA) curves of the developed composites are presented in Figure 5. The unfilled PLA/PBAT blend displayed the highest initial resistance to thermal degradation, with a 5% mass-loss temperature (T5%) of approximately 312°C. Incorporation of 20 wt.% untreated corn-husk fiber reduced T5% to approximately 297°C because lignocellulosic constituents possess lower thermal stability than the polyester matrix.

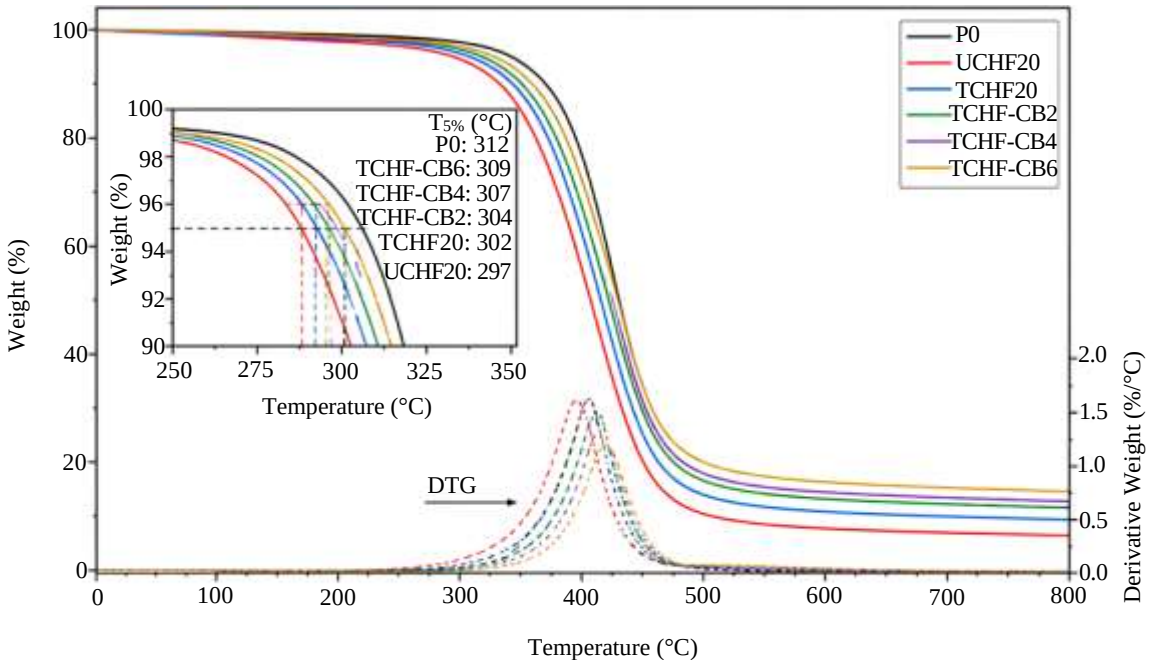


Figure 5. TGA curves illustrating the influence of corn husk fiber treatment and carbon-black concentration on thermal degradation behavior.

In particular, hemi-cellulose and residual low-molecular-weight surface components can begin to decompose at lower temperatures, leading to earlier mass loss in the untreated-fiber composite. Alkaline treatment increased T5% from approximately 297°C for UCHF20 to 302°C for TCHF20. The improvement can be attributed to the partial removal of thermally less stable hemicellulose, waxes and other surface impurities during NaOH treatment. The treated fibers, therefore, introduced a smaller low-temperature degradation contribution while retaining the cellulose-rich reinforcing framework.

Carbon-black incorporation produced a further gradual improvement in the initial degradation resistance of the treated-fiber composites. T5% increased to approximately 304°C for TCHF-CB2, 307°C for TCHF-CB4 and 309°C for TCHF-CB6. The thermally stable carbonaceous phase can hinder polymer-chain mobility and increase the tortuosity of diffusion pathways for volatile degradation products [15]. At higher temperature, the residual mass would also be expected to increase with CB loading because the conductive carbon phase does not volatilize within the principal polymer degradation interval.

© STM Journals 2026. All Rights Reserved

Although the CHF-containing formulations exhibited somewhat lower thermal stability than the unfilled PLA/PBAT blend, all compositions retained a wide margin between the injection-moulding temperature of approximately 175-185°C and the onset of major thermal decomposition. For the optimized TCHF-CB4 formulation, the representative T5% value of approximately 307°C provides a thermal processing window exceeding 120°C relative to the upper moulding temperature. This indicates that the composite can be processed by conventional melt-compounding and injection-moulding routes without approaching the principal degradation region, provided that moisture is adequately removed from both the polyester matrix and the lignocellulosic reinforcement before processing.

Although the selected melt-processing temperatures are substantially lower than the principal degradation temperatures measured by TGA, the possibility of limited thermal or hydrolytic modification of the individual constituents should be considered. Lignocellulosic reinforcement contains hemicellulose, lignin and other low-molecular-weight components that are less thermally stable than the polyester matrix, whereas PLA/PBAT-based matrices can undergo molecular-weight reduction in the presence of residual moisture during melt processing. For this reason, both the polymer pellets and corn husk fibers were thoroughly dried before compounding, and the processing temperature was restricted to a maximum of approximately 185°C. The optimized TCHF-CB4 composite exhibited a T5% of approximately 307°C, providing a processing-to-degradation temperature margin greater than 120°C. Therefore, severe bulk thermal degradation is unlikely under the adopted conditions, although minor molecular-level changes cannot be completely excluded solely from TGA data. Control of moisture content, melt residence time and processing temperature is consequently important for maintaining the integrity of both the lignocellulosic reinforcement and the PLA/PBAT matrix.

Mechanical Performance

The mechanical response of the developed composites was evaluated in terms of tensile strength, tensile modulus, elongation at break, flexural strength and notched impact strength. The representative mechanical properties are summarized in Table 3 and illustrated in Figures 6–8. The results demonstrate that the overall mechanical behavior is governed by the combined effects of fiber-matrix interfacial adhesion, the stiffening contribution of corn husk fiber, the ductile PBAT phase and the progressive formation of a rigid carbon-black network.

Table 3. Mechanical properties of the developed composites.

Composite	Tensile strength (MPa)	Tensile modulus (GPa)	Elongation at break (%)	Flexural strength (MPa)	Notched impact strength (kJ m^{-2})
P0	42.8	2.10	25.6	61.4	30.7
UCHF20	38.5	2.96	6.4	64.8	20.9
TCHF20	47.6	3.25	7.1	75.8	26.1
TCHF-CB2	46.8	3.39	6.5	74.9	25.0
TCHF-CB4	45.9	3.58	5.8	72.6	23.8
TCHF-CB6	42.3	3.76	4.9	69.1	20.5

Tensile Strength and Interfacial Efficiency

The unfilled PLA/PBAT blend (P0) exhibited a tensile strength (Figure 6) of approximately 42.8 MPa. Incorporation of 20 wt.% untreated corn husk fiber decreased the tensile strength to approximately 38.5 MPa, corresponding to a reduction of about 10%.

This decrease indicates that the reinforcing ability of corn husk fiber cannot be assessed solely from its intrinsic stiffness. When the fiber-matrix interface is weak, the interface becomes the preferred location for crack initiation and propagation under tensile loading [16].

© STM Journals 2026. All Rights Reserved

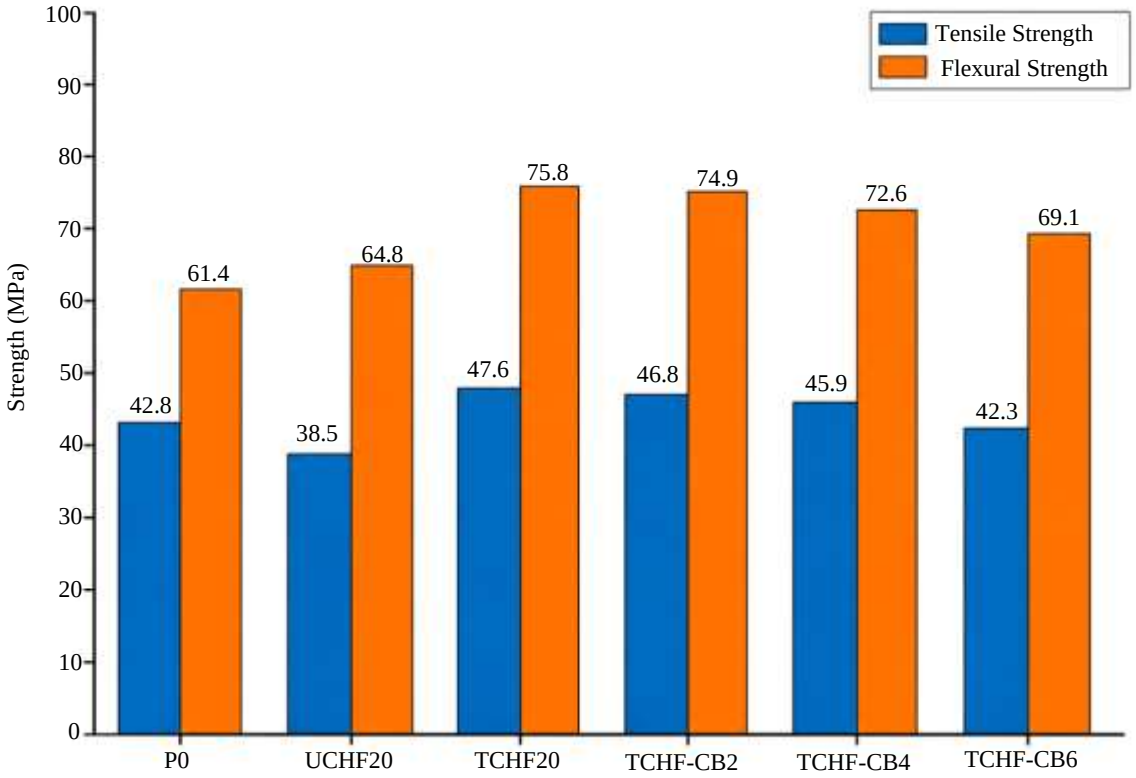


Figure 6. Tensile and flexural strength of the developed composites.

The untreated corn husk fiber contains a comparatively hydrophilic surface enriched with hydroxyl-containing lignocellulosic constituents, while residual waxes, hemicellulose and loosely bound lignin can further limit effective wetting by the polyester-rich matrix. Consequently, interfacial debonding and fiber pull-out are promoted, restricting efficient stress transfer from the PLA/PBAT matrix to the reinforcing phase.

Following alkaline treatment, the tensile strength increased markedly to approximately 47.6 MPa for TCHF20. This represents an increase of about 23.6% relative to UCHF20 and approximately 11.2% relative to the unfilled P0 blend. The improvement confirms the beneficial effect of fiber surface modification. Partial removal of weak surface constituents, together with the increase in fiber roughness and fibrillation, enhances mechanical interlocking and improves fiber wetting during melt processing, allowing a greater proportion of the applied load to be transferred to the fiber.

The incorporation of 2 wt.% carbon black caused only a minor reduction in tensile strength to approximately 46.8 MPa, indicating that low conductive-filler loading did not significantly disturb the reinforced polymer network [16–19]. The TCHF-CB4 formulation retained a tensile strength of approximately 45.9 MPa, corresponding to about 96.4% of the tensile strength of TCHF20, while simultaneously developing stable electrical conductivity and piezoresistive functionality. At 6 wt.% CB, the present results indicate stronger filler–filler interactions and a substantially denser conductive network than at 4 wt.% CB. However, because the detailed SEM analysis presented here primarily characterizes the optimized TCHF-CB4 formulation, extensive carbon-black agglomeration in TCHF-CB6 cannot be established conclusively from morphology alone. The reduction in tensile and impact strength at 6 wt.% CB, together with the marked reduction in electrical resistivity and sensing gauge factor, is nevertheless consistent with increased network densification and possible localized CB clustering. Such locally concentrated particulate regions can increase matrix constraint and act as stress-concentration sites. Accordingly, the term “agglomeration” is used here as a plausible interpretation of the combined mechanical and electrical trends rather than as a quantitatively verified morphological feature.

© STM Journals 2026. All Rights Reserved

Tensile Modulus

In contrast to tensile strength, the tensile modulus (Figure 7) increased almost continuously with the addition of rigid solid phases. P0 exhibited a modulus of approximately 2.10 GPa. Addition of untreated CHF increased the modulus to approximately 2.96 GPa because the lignocellulosic fiber possessed a higher stiffness than the surrounding polymer blend and restricted matrix deformation.

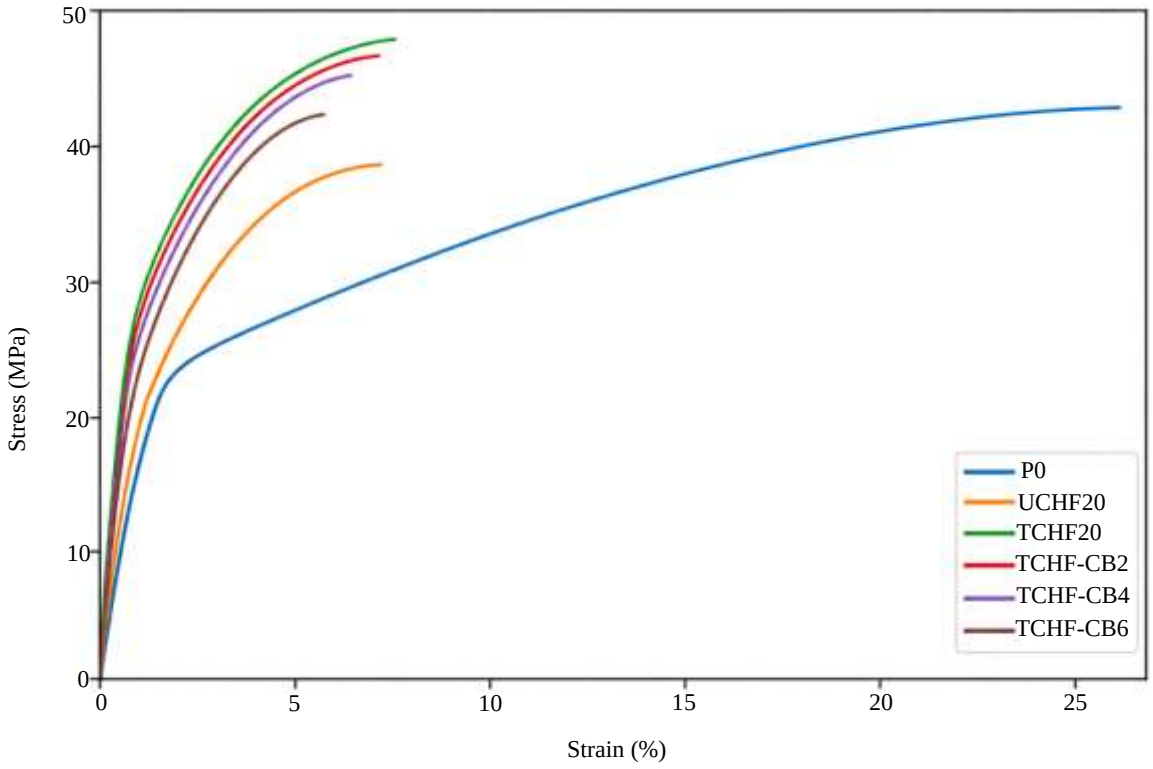


Figure 7. Representative tensile modulus showing progressive stiffening with CHF and CB incorporation.

Alkaline treatment further increased the modulus to approximately 3.25 GPa. Improved fiber-matrix adhesion allows the stiffness of the reinforcement to contribute more effectively to the macroscopic composite response, because interfacial slip is reduced and the applied stress is transmitted more efficiently across the fiber-polymer boundary.

Carbon-black incorporation produced an additional progressive stiffening effect. The tensile modulus increased to approximately 3.39, 3.58 and 3.76 GPa for TCHF-CB2, TCHF-CB4 and TCHF-CB6, respectively. The modulus of TCHF-CB4 was, therefore, about 70.5% higher than that of P0. This behavior is associated with restricted polymer-chain mobility in the presence of the rigid particulate phase and increasing filler-filler interactions as the CB concentration approaches and exceeds the conductive percolation region [20]. The resulting increase in stiffness is advantageous for thin-wall consumer-electronics casings, where dimensional rigidity and resistance to flexural deformation are important.

Flexural Behavior

The flexural response (Figure 8) followed a trend like the tensile strength, although the stiffening influence of the fiber was more evident under bending. P0 exhibited a flexural strength of approximately 61.4 MPa, while incorporation of untreated CHF increased the value moderately to about 64.8 MPa. Although UCHF20 showed a decrease in tensile strength, its flexural strength increased because the rigid fiber phase contributed to resistance against bending deformation even when the interface was not sufficiently strong to maximize tensile load transfer.

© STM Journals 2026. All Rights Reserved

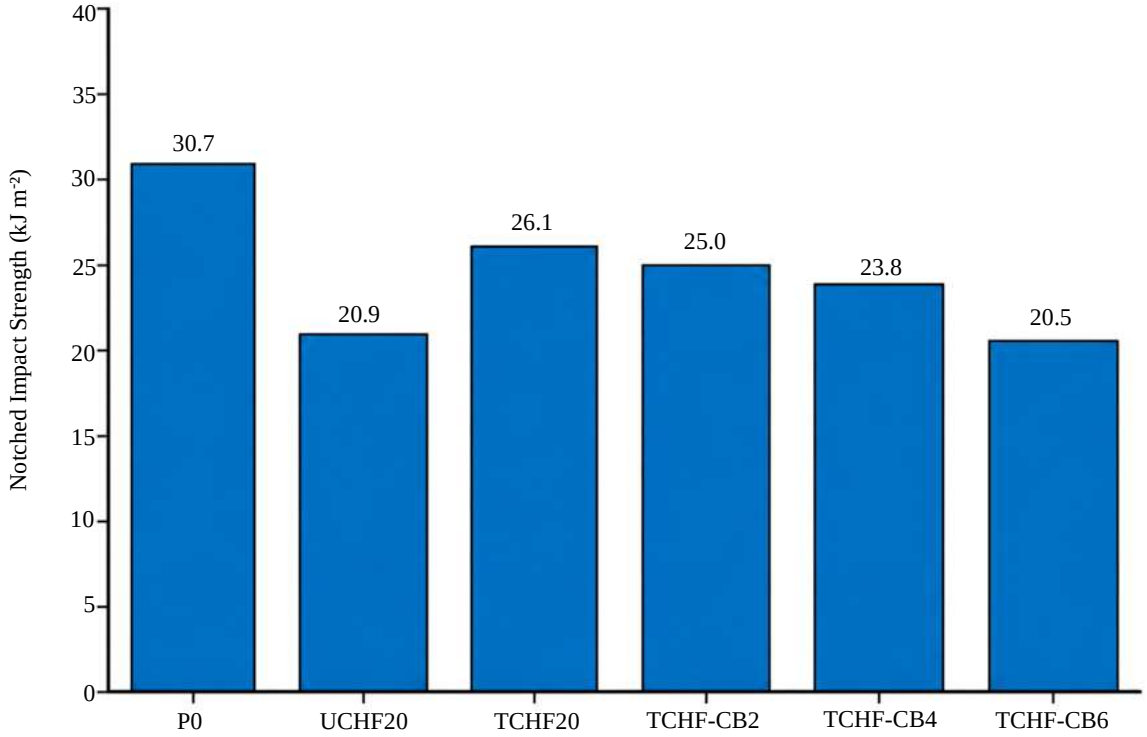


Figure 8. Notched impact strength of the developed composites.

Alkali-treated fiber produced a much greater improvement. TCHF20 achieved a flexural strength of approximately 75.8 MPa, representing an increase of about 23.5% relative to P0. During three-point bending, the outer surface of the specimen experiences tensile stress while the inner surface is subjected to compression. Improved adhesion between treated CHF and the PLA/PBAT matrix enables more efficient transfer of these stresses and delays fiber–matrix separation, thereby increasing the load required for flexural failure.

The addition of CB caused a gradual decrease in flexural strength after the optimum treated-fiber condition, but the values remained higher than those of P0. TCHF-CB2 and TCHF-CB4 exhibited flexural strengths of approximately 74.9 and 72.6 MPa, respectively, while TCHF-CB6 showed approximately 69.1 MPa [21]. Thus, TCHF-CB4 maintained a flexural strength about 18.2% higher than the unfilled PLA/PBAT blend while providing self-sensing functionality. This result confirms that the conductive filler concentration required for piezoresistive behavior did not eliminate the structural reinforcement provided by the treated corn husk fiber.

Impact Resistance and Toughness

Impact behavior (Figure 9) differed from the stiffness-related properties because the ability of the material to absorb rapid mechanical energy depends strongly on matrix ductility, interfacial debonding mechanisms and the presence of local stress concentrators. P0 exhibited the highest representative impact strength of approximately 30.7 kJ m^{-2}. The relatively high impact resistance of the unfilled blend can be attributed mainly to the PBAT phase, which promotes plastic deformation and dissipates impact energy within the PLA-rich matrix.

The incorporation of untreated CHF decreased impact strength markedly to approximately 20.9 kJ m^{-2}. Poorly bonded fiber ends and interfacial voids act as preferential sites for crack initiation, while weak fiber–matrix boundaries provide a comparatively low-energy path for crack propagation. Consequently, the stiffening achieved by untreated fiber was accompanied by a substantial loss of impact toughness.

© STM Journals 2026. All Rights Reserved

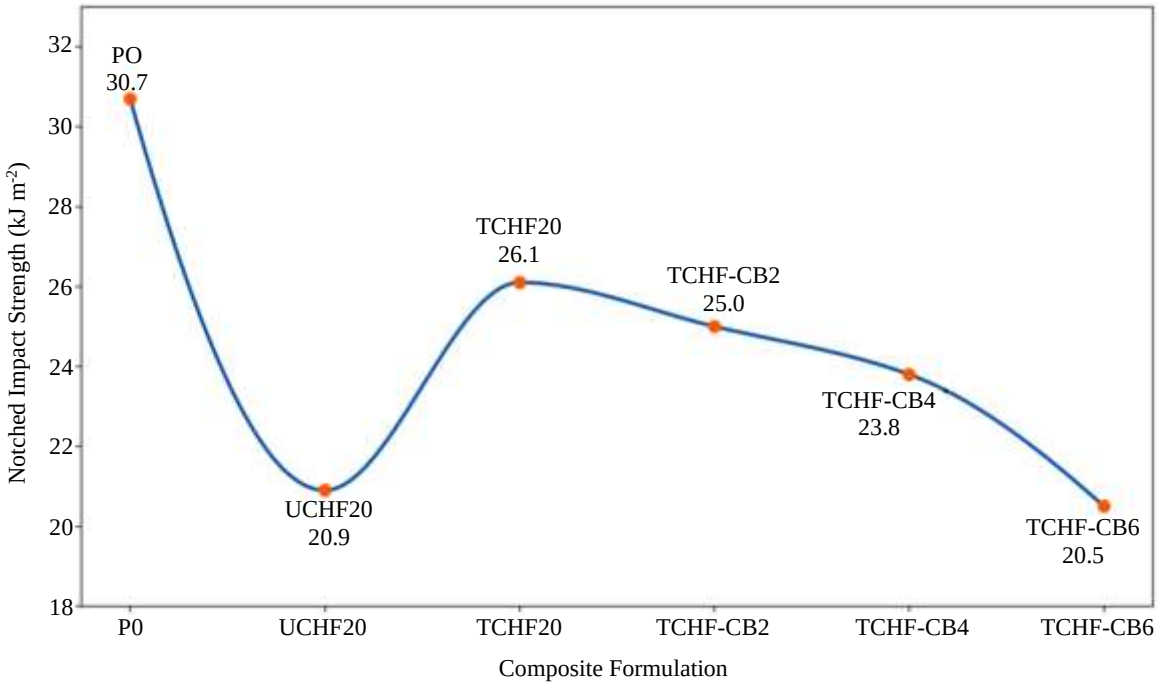


Figure 9. Notched impact strength variation of the developed PLA/PBAT–corn husk composites.

Alkaline treatment recovered a significant proportion of the lost impact resistance, increasing the value to approximately 26.1 kJ m^{-2} for TCHF20. This corresponds to an improvement of nearly 25% relative to UCHF20. The stronger interface forces propagating cracks to follow more complex paths involving fiber fracture, crack deflection, matrix deformation and frictional energy dissipation, thereby increasing the energy required for failure [21, 22].

Progressive addition of CB reduced impact resistance. TCHF-CB2 and TCHF-CB4 exhibited impact strengths of approximately 25.0 and 23.8 kJ m^{-2}, respectively, whereas TCHF-CB6 decreased to about 20.5 kJ m^{-2}. Increasing carbon-black loading restricts local polymer deformation and can generate rigid agglomerates that act as stress concentrators during high-rate loading. The approximately 22.5% decrease in the impact strength of TCHF-CB4 relative to P0 must, therefore, be considered together with its substantial increase in modulus, improved flexural strength and acquisition of electrical self-sensing capability. The optimized composite is consequently defined by a balanced multifunctional response rather than by maximum impact toughness alone.

Electrical Percolation Behavior

The electrical properties (Figure 10) exhibited a fundamentally different dependence on carbon-black concentration from the mechanical properties. The treated corn husk fiber composite without conductive filler remained electrically insulating, with a representative volume resistivity greater than $10^{10}\Omega$ cm. This behavior confirms that the PLA/PBAT matrix and lignocellulosic reinforcement do not themselves provide a continuous electron-conduction pathway and that electrical functionality is introduced primarily through the carbon-black phase.

At 2 wt.% CB, the volume resistivity decreased to approximately 3.4×10^{10} Ω cm. Although this represents a substantial reduction relative to TCHF20, the material remained within a pre-percolation regime. At this concentration, conductive particles predominantly existed as isolated aggregates separated by polymer-rich regions, and electron transport depended on a limited number of long-range tunnelling events [23]. Consequently, stable low-resistance pathways were not yet fully established.

© STM Journals 2026. All Rights Reserved

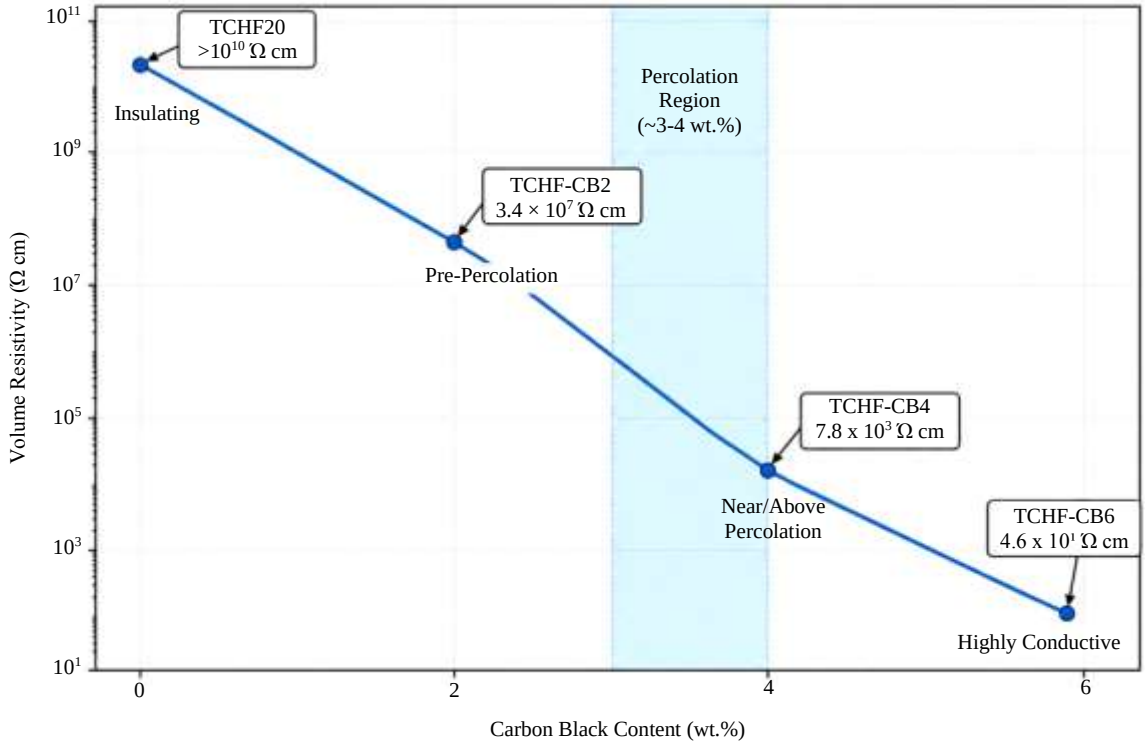


Figure 10. Electrical percolation behavior of the PLA/PBAT–corn husk composites as a function of carbon-black content.

A much more pronounced transition occurred when the CB content increased to 4 wt.%. The representative resistivity decreased to approximately 7.8×10^3 Ω cm, corresponding to a reduction of nearly four orders of magnitude compared with the 2 wt.% formulation. Such a sharp change is characteristic of electrical percolation and indicates that the average interparticle separation had decreased sufficiently for direct contacts and short-range tunnelling pathways to form a system-spanning conductive network.

Increasing the filler content further to 6 wt.% reduced the resistivity to approximately 4.6×10^1 Ω cm. The composite at this concentration was, therefore, strongly conductive compared with the 4 wt.% composition. Nevertheless, the increase in absolute conductivity did not provide an equivalent improvement in self-sensing sensitivity, because the dense network contained numerous redundant current pathways.

The comparatively low percolation region of approximately 3–4 wt.% CB can be associated with the high specific surface area of carbon black together with its preferential localization within polymer-rich zones and near interphase boundaries. Such selective spatial distribution reduces the quantity of conductive filler required to create a continuous network. In the present hybrid architecture, the treated CHF phase also constrains the available polymer volume and may indirectly increase the local CB concentration within the continuous matrix regions.

Table 4. Electrical and self-sensing characteristics.

Composite	Volume resistivity (Ω cm)	Conductive state	Gauge factor	Cyclic behavior
TCHF20	$>10^{10}$	Insulating	–	Not measurable.
TCHF-CB2	3.4×10^7	Pre-percolation	Unstable	Noisy/discontinuous.
TCHF-CB4	7.8×10^3	Near/above percolation	4.8	Stable.
TCHF-CB6	4.6×10^1	Highly conductive	2.6	Stable but less sensitive.

© STM Journals 2026. All Rights Reserved

The electrical results, therefore, identify TCHF-CB4 as the first formulation possessing a sufficiently stable conductive network for reliable resistance measurement. This composition lies sufficiently above the percolation threshold to avoid discontinuous electrical response while remaining close enough to the transition region to preserve a strong dependence of resistance on mechanical deformation. The electrical data, therefore, demonstrate conductive-network densification above the percolation threshold, but do not by themselves distinguish uniformly distributed additional conductive contacts from localized CB agglomeration. A quantitative assessment of CB cluster size and spatial distribution using high-resolution SEM/TEM and image analysis would be valuable in future work to establish the agglomeration threshold independently of electrical percolation.

Piezoresistive Response Under Tensile Deformation

The representative relationship between applied tensile strain and normalized resistance change ($\Delta R/R_0$) for TCHF-CB4 and TCHF-CB6 is shown in Figure 11. For the 4 wt.% CB composite, $\Delta R/ R_0$ increased progressively with increasing strain and displayed an approximately linear response in the low-strain region.

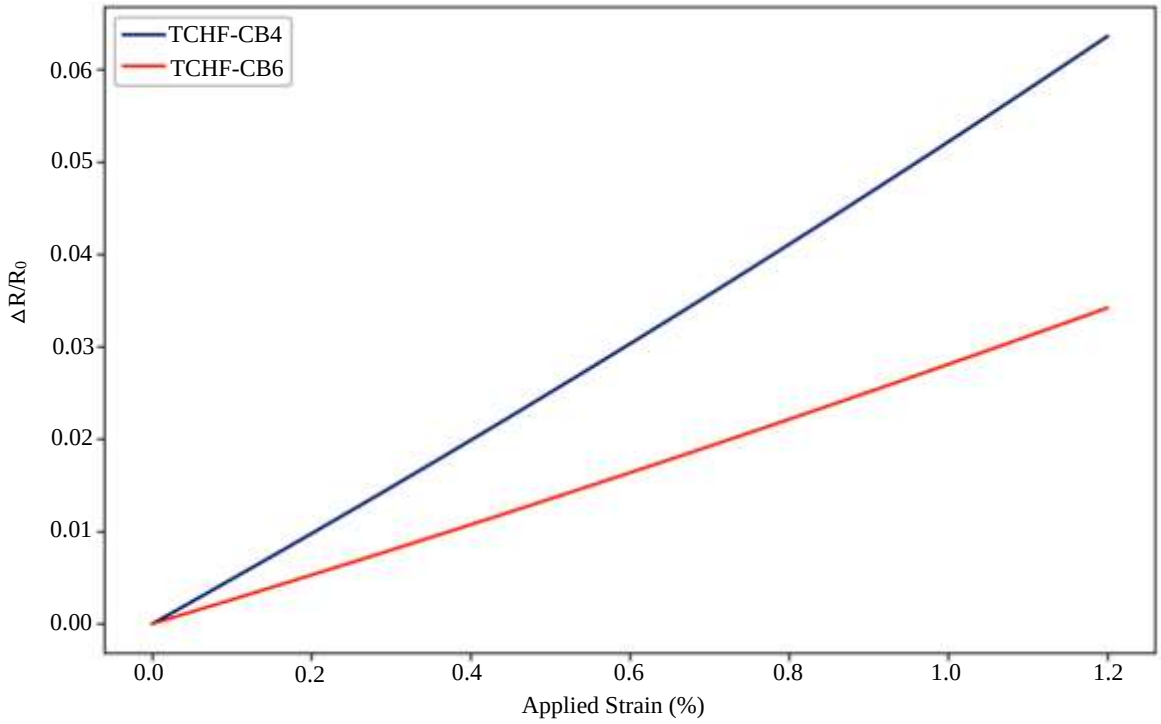


Figure 11. Representative normalized resistance changes as a function of applied tensile strain for TCHF-CB4 and TCHF-CB6.

From this region, a representative gauge factor of approximately 4.8 was obtained, indicating that the electrically percolated composite was sufficiently sensitive to small deformation for self-sensing applications. The origin of the piezoresistive response is closely related to deformation of the carbon-black network embedded within the thermoplastic matrix. Fundamentally, the piezoresistive behavior can be described as a coupled contact–tunnelling mechanism operating within a strain-sensitive percolated CB network. Electrical transport occurs through both direct physical contacts among neighboring carbon-black aggregates and quantum tunnelling across thin insulating polymer gaps. The tunnelling resistance may be represented qualitatively as

$$R_t \propto \exp(\beta d)$$

where R□ is the tunnelling resistance, d is the separation distance between neighboring conductive aggregates, and β is a parameter related to the barrier characteristics of the intervening polymer.

© STM Journals 2026. All Rights Reserved

Consequently, a small strain-induced increase in d can cause a disproportionately large increase in tunnelling resistance. Simultaneously, deformation may break some direct CB–CB contacts, decreasing the number of continuous conductive pathways through the composite. The combined loss of direct contacts and increase in tunnelling distance, therefore, increases the macroscopic electrical resistance during loading. During unloading, elastic and viscoelastic recovery of the PLA/PBAT matrix reduces interparticle spacing and restores a substantial fraction of the conductive network, resulting in partial or nearly complete resistance recovery.

Sensitivity is maximized near the electrical percolation threshold because macroscopic conduction is controlled by a relatively small number of critical pathways. In TCHF-CB4, which lies close to the approximately 3–4 wt.% percolation region, deformation of only a limited number of contacts substantially alters total resistance, resulting in a gauge factor of approximately 4.8. In contrast, TCHF-CB6 contains a denser network with numerous parallel and redundant conductive paths. Disruption of individual contacts, therefore, produces a smaller fractional resistance change, explaining the lower gauge factor of approximately 2.6 despite its substantially higher electrical conductivity. Thus, the observed piezoresistive response is fundamentally governed by strain-induced modulation of contact conduction and electron tunnelling within a near-percolated carbon-black network.

When tensile strain is applied, the PLA/PBAT phase undergoes elastic and viscoelastic deformation, increasing the average separation between neighboring CB aggregates. Some direct particle-to-particle contacts are disrupted, while the tunnelling distance between other neighboring aggregates increases. Because electrical tunnelling probability decreases strongly with increasing separation distance, both mechanisms contribute to an increase in measured resistance [22, 23].

Upon unloading, elastic recovery of the surrounding polymer decreases the interparticle distance and allows a substantial fraction of the conductive pathways to reform. The resistance, therefore, approaches its initial value, producing a reversible electrical response at low deformation. This mechanism is particularly attractive for smart casings because the sensing function originates from the same bulk material that carries the mechanical load rather than from a separately bonded sensor.

The TCHF-CB6 formulation exhibited a lower representative gauge factor of approximately 2.6 despite its much lower initial resistivity. At 6 wt.% CB, a dense network of conductive particles exists throughout the polymer-rich phase. The presence of numerous parallel conduction pathways means that disruption of a limited number of contacts during deformation produces only a relatively small change in the overall electrical resistance.

In contrast, the TCHF-CB4 composition remains close to the percolation region, where the number of available conductive pathways is comparatively limited. Small microstructural changes can, therefore, interrupt a significant proportion of the total network, producing a larger relative change in resistance. This result demonstrates that maximum electrical conductivity and maximum sensing sensitivity do not occur at the same filler concentration. For self-sensing polymer composites, an optimum filler level should provide stable percolation without creating excessive conductive-network redundancy.

Cyclic Piezoresistive Response and Sensing Repeatability

The cyclic piezoresistive response of the optimized TCHF-CB4 composition is illustrated in Figure 12. During each flexural loading cycle, the normalized resistance increased as the specimen deformed and decreased during unloading.

The close correspondence between the imposed mechanical cycle and the electrical response confirms that rearrangement of the conductive carbon-black network was repeatedly coupled to

© STM Journals 2026. All Rights Reserved

deformation of the polymer composite. A small baseline shift can occur during the initial conditioning cycles. Such behavior is consistent with the heterogeneous and viscoelastic nature of conductive thermoplastic composites and can arise from several concurrent processes, including polymer-chain relaxation, microscopic redistribution of CB aggregates, stabilization of tunnelling distances, local adjustment at fiber–matrix interfaces and stabilization of the electrode–specimen contact. After this initial accommodation, successive electrical cycles became comparatively reproducible.

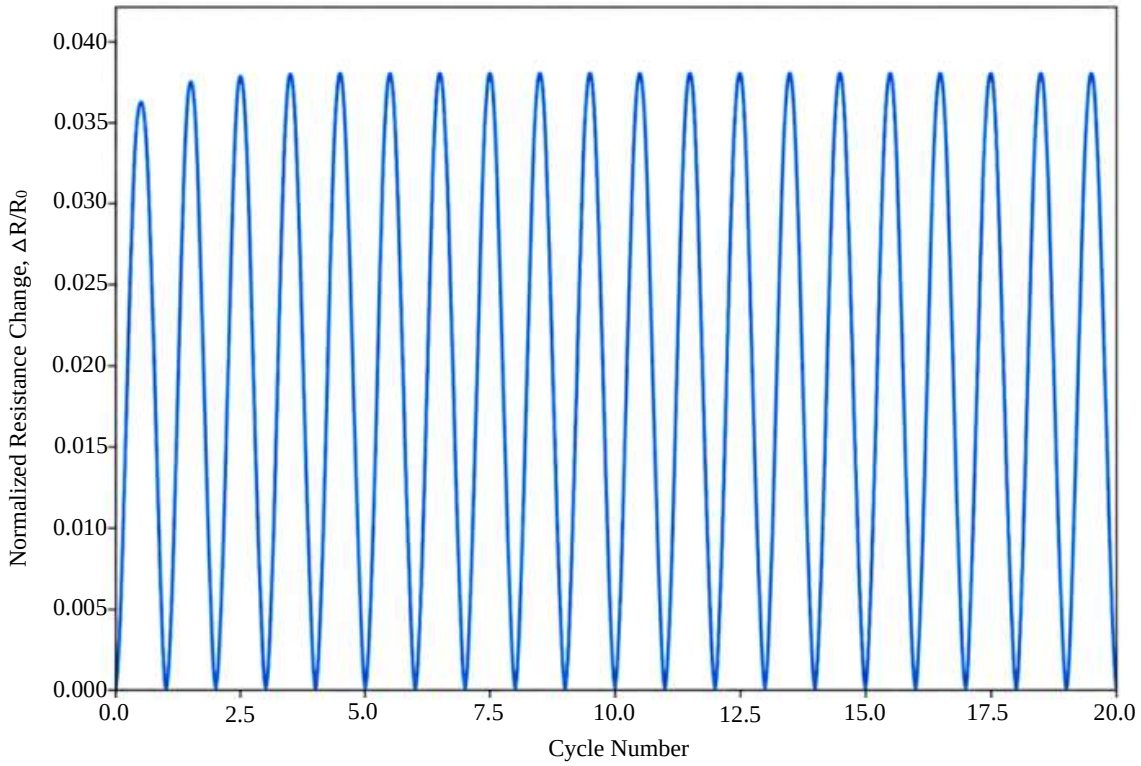


Figure 12. Piezoresistive response of TCHF-CB4 under repeated flexural deformation.

For the representative response, the residual drift after extended cycling remained approximately 4.3%, indicating adequate short-term repeatability for low-cost deformation monitoring. The repeated formation and disruption of conductive pathways did not lead to immediate electrical failure, suggesting that the CB network possessed sufficient connectivity to tolerate reversible strain while maintaining a measurable resistance signal [23].

The ability to generate a repeatable signal without an externally bonded strain gauge is a key advantage of the proposed composite architecture. Since the conductive phase is distributed through the casing material, deformation within the electrically active region directly perturbs the internal network. This eliminates additional sensor bonding operations and can simplify the construction of low-cost smart housings.

Reversible Deformation and Damage-Sensitive Resistance Response

At relatively low strain, most changes in the conductive-network geometry are reversible. The polymer matrix recovers after removal of the load, allowing neighboring carbon-black aggregates to return close to their original separation distances. Consequently, the measured resistance returns close to its initial baseline. This reversible response is suitable for detecting temporary bending, handling deformation or moderate mechanical loading of the casing.

At higher deformation levels, however, permanent microstructural changes can occur. These may include local fiber–matrix debonding, plastic deformation of PBAT-rich regions, microcrack

© STM Journals 2026. All Rights Reserved

development in the PLA-rich phase, fiber fracture and irreversible separation of neighboring CB aggregates. Because such damage prevents full restoration of the original conductive network, the electrical resistance may retain a permanent offset after unloading.

This behavior provides the composite with two complementary sensing modes. Reversible changes in resistance can indicate recoverable deformation, whereas an irreversible baseline shift can act as a simple indicator of overload or structural damage. In a consumer-electronics casing, such a response could potentially identify excessive bending, crushing, impact-related micro-damage or localized deformation around fasteners and assembly features.

CONCLUSIONS

The present study demonstrates that a multifunctional natural–fiber-reinforced thermoplastic polymer composite can be engineered by combining a PLA/PBAT matrix, alkali-treated corn husk reinforcement, and a carbon-black conductive phase. The resulting polymer-composite behavior was governed by fiber–matrix interfacial quality, filler dispersion, polymer crystallization, mechanical reinforcement, and conductive-network formation. The principal conclusions are as follows:

- Alkali treatment modified the corn husk fiber surface by removing part of the non-cellulosic constituents and increasing surface roughness and fibrillation. This promoted improved wetting, mechanical interlocking, and interfacial stress transfer between the lignocellulosic reinforcement and the PLA/PBAT polymer matrix.
- Incorporation of CHF and CB strongly influenced the thermal and crystalline characteristics of the polymer composite. PLA cold-crystallization temperature decreased from 112.5°C for P0 to 102.4°C for TCHF-CB6, while crystallinity increased from 17.2% to 32.1%, confirming the heterogeneous nucleating effect of both fibrous and particulate phases.
- Fiber surface modification significantly enhanced the mechanical efficiency of the polymer composite. Tensile strength increased from 38.5 MPa for UCHF20 to 47.6 MPa for TCHF20, demonstrating that improved fiber–matrix adhesion was more important than fiber incorporation alone for effective reinforcement.
- The hybrid TCHF-CB4 composite provided a favorable structural balance, with a tensile strength of 45.9 MPa, tensile modulus of 3.58 GPa, flexural strength of 72.6 MPa, and notched impact strength of 23.8 kJ m^{-2}. These values confirm that conductive filler incorporation retained useful load-bearing capability within the reinforced thermoplastic matrix.
- Carbon-black incorporation converted the insulating fiber-reinforced polymer composite into an electrically conductive multifunctional system. Volume resistivity decreased from $>10^{10}$ Ω cm for TCHF20 to 7.8×10^3 Ω cm for TCHF-CB4, with electrical percolation occurring near 3–4 wt.% CB.
- Among the investigated polymer composites, TCHF-CB4 exhibited the best structural-functional balance, combining reinforced mechanical behavior, enhanced crystallinity, adequate thermal stability, stable conductive percolation, a gauge factor of 4.8, and approximately 4.3% residual drift during cyclic deformation. The developed material, therefore, represents a promising multifunctional polymer composite in which the thermoplastic matrix, natural-fiber reinforcement, and conductive filler act synergistically to provide structural support and intrinsic self-sensing capability.

REFERENCES

1. Sztorch B, Brząkalski D, Pakuła D, Frydrych M, Špitalský Z, Przekop RE. Natural and synthetic polymer fillers for applications in 3D printing—FDM technology area. Solids. 2022;3(3):508–548.
2. Sandanamsamy L, Harun WS, Ishak I, Romlay FR, Kadirgama K, Ramasamy D, et al. A comprehensive review on fused deposition modelling of polylactic acid. Prog Addit Manuf. 2023;8(5):775–799.
3. Aigbodion VS, Okonkwo EG, Akinlabi ET. Eco-friendly polymer composite: State-of-Arts, Opportunities and Challenge. In: Sustainable Polymer Composites and Nanocomposites. Cham: Springer International Publishing; 2019 Feb 2. p. 1233–1265.
4. Jayanth D, Kumar PS, Nayak GC, Kumar JS, Pal SK, Rajasekar R. A review on biodegradable polymeric materials striving towards the attainment of green environment. J Polym Environ. 2018;26(2):838–865.

© STM Journals 2026. All Rights Reserved

5. Boey JY, Lee CK, Tay GS. Factors affecting mechanical properties of reinforced bioplastics: A review. Polymers. 2022;14(18):3737.
6. Samir A, Ashour FH, Hakim AA, Bassyouni M. Recent advances in biodegradable polymers for sustainable applications. npj Mater Degrad. 2022;6(1):68.
7. Asyraf MR, Rafidah M, Azrina A, Razman MR. Dynamic mechanical behaviour of kenaf cellulosic fibre biocomposites: A comprehensive review on chemical treatments. Cellulose. 2021;28(5):2675–2695.
8. Jani HR, Essassi FE, Mahbub M, Rahman AS, Tarafder S. FDM Based 3D Printing of Short Fiber Composites: A Comparative Review of Synthetic and Natural Fiber Composites.
9. Sun Y, Zheng Z, Wang Y, Yang B, Wang J, Mu W. PLA composites reinforced with rice residues or glass fiber—A review of mechanical properties, thermal properties, and biodegradation properties. J Polym Res. 2022;29(10):422.
10. Girisha L, Saravanan R, Kumarasan T, Pitchandi P, Sakthi S, Nanthakumar S, et al. Hemp fibre-reinforced polylactic acid composites: A Sustainable Materials for Engineering and Industry. In: Polymer Composites: Fundamentals and Applications. Singapore: Springer Nature Singapore; 2024 May 4. p. 217–248.
11. Ibrahim MI, Sapuan SM, Zainudin ES, Zuhri MY. Potential of using multiscale corn husk fiber as reinforcing filler in cornstarch-based biocomposites. Int J Biol Macromol. 2019 Oct 15;139:596–604.
12. Ibrahim MI, Sapuan SM, Zainudin ES, Zuhri MY. Preparation and characterization of cornhusk/sugar palm fiber reinforced cornstarch-based hybrid composites. J Mater Res Technol. 2020;9(1):200–211.
13. Hasan MH, Islam S, Sajib MS, Rahman GS, Sabur MA, Ahmed AN, et al. A comprehensive study of agricultural waste maize husk as a potential reinforcement in maize fiber/glass fiber hybrid composites. SPE Polym. 2025 Apr;6(2):e70000.
14. Kwon HJ, Sunthornvarabhas J, Park JW, Lee JH, Kim HJ, Piyachomkwan K, et al. Tensile properties of kenaf fiber and corn husk flour reinforced poly (lactic acid) hybrid bio-composites: Role of Aspect Ratio of Natural Fibers. Compos Part B Eng. 2014 Jan 1;56:232–237.
15. Sani A, Inuwa IM, Mustapha HM, Yunana EU, Abubakar M. Tensile, flexural, impact, hardness and structural characterization of coir fiber/maize husk hybrid composites for electrical fittings. Sci World J. 2025;20(1):341–355.
16. Sari NH, Fajrin J, Fudholi A. Characterisation of swellability and compressive and impact strength properties of corn husk fibre composites. Composites Communications. 2020 Apr 1;18:49-54.
17. Youssef AM, El-Gendy A, Kamel S. Evaluation of corn husk fibers reinforced recycled low density polyethylene composites. Mater Chem Phys. 2015 Feb 15;152:26–33.
18. Yuvaraj G, Ramesh M. Mechanical, wear, and hydrophobic properties of silane-treated corn husk fibre and betel nut epoxy composites. Biomass Convers Biorefin. 2023;13(16):15227–15234.
19. Balasubramanian E, Subramaniyan K, Sankar SK, Pazhani N. Nanoclay influence on hygrothermal aging of corn husk–glass fiber hybrid composites. J Reinf Plast Compos. 2026 Jan 30:073168 44261418344.
20. Sari NH, Suteja S, Sutaryono YA, Sujita S, Syafri E. Evaluation of hybrid corn husk fiber/Hibiscus tiliaceus fiber powders–reinforced coconut shell/polyester composites: Effect of Volume Fraction on Mechanical and Morphological Properties. In: Emerging Sustainable and Renewable Composites. CRC Press; 2024 Jul 3. p. 53–69.
21. Sari NH, Suteja S, Ilyas RA, Syafri E, Indran S. Characterization of the density and mechanical properties of corn husk fiber reinforced polyester composites after exposure to ultraviolet light. Funct Compos Struct. 2021;3(3):034001.
22. Sari NH, Suteja S, Fudholi A, Sutaryono YA, Maskur M, Srisuk R, et al. Evaluation of impact, thermo-physical properties, and morphology of cornhusk fiber-reinforced polyester composites. Polym Compos. 2022;43(5):2771–2778.
23. Alomaja JA, Jimoh AA, Joseph OP, Wilson UN. Flexural and tensile properties of chemically treated guinea corn husk-cow hair hybrid fiber reinforced cement composite. Mater Today Proc. 2023;86:77–81.

© STM Journals 2026. All Rights Reserved